Plasmons in periodic solids

K. C. Pandey,* P. M. Platzman, and P. Eisenberger
Bell Laboratories, Murray Hill, New Jersey 07974

E-Ni Foo
Drexel University, Philadelphia, Pennsylvania 19104

(Received 24 January 1974)

Within the framework of the random-phase approximation we consider the effect of band structure on characteristic-energy-loss experiments.

I. INTRODUCTION

Recent experimental work[1] utilizing x rays to probe the dynamic structure factor $S(\vec{q}, \omega)$ of simple metals has demonstrated the existence of crystal potential effects in the spectrum of these materials. Theoretical work on this matter is extremely limited. Generally the calculations[2] which have been published concentrate on the detailed numerical evaluations of the diagonal components of the frequency- and wave-vector-dependent dielectric tensor. In this work the emphasis will be on an over-all understanding of the role of band structure in characteristic-energy-loss experiments. We will show how the random-phase-approximation (RPA) expressions with band structure (RPAB) may, at high frequencies, be simplified and the essential physics of the periodic potential elucidated. Utilizing some elementary models of the band structure, we may evaluate the important formulas to quantitatively predict the general properties of the characteristic loss spectrum within the RPAB approximation.

The experimental spectrum, while qualitatively displaying the predicted behavior, is not in good quantiative agreement with these results. In addition to our general discussion, we will present some numerical calculations relevant to a simple two-band model.[3]

II. CROSS SECTION

In a typical x-ray scattering experiment (Fig. 1) the spectrum of x rays scattered through a fixed angle θ with momentum transfer $|\vec{q}| \approx 2|\vec{k}_1| \sin(\frac{1}{2}\theta)$ and energy loss $\omega = \omega_1 - \omega_2$ is given by[4]

$$\frac{d^2\sigma}{d\omega\, d\Omega} = \left(\frac{d\sigma}{d\Omega}\right)_0 \left(\frac{\omega_2}{\omega_1}\right) \frac{|\vec{q}|^2}{4\pi^2 e^2} \operatorname{Im}\left(\frac{1}{\epsilon(\vec{q}, \omega)}\right), \quad (1)$$

where $(d\sigma/d\Omega)_0$ is the well-known Thomson cross section and $\epsilon^{-1}(\vec{q}, \omega)$ is formally defined in terms of the response of the system to an external longitudinal potential $\varphi_{\text{ext}}(\vec{q}, \omega)$, i.e.

$$\epsilon^{-1}(\vec{q}, \omega) \equiv \varphi_{\text{total}}(\vec{q}, \omega)/\varphi_{\text{ext}}(\vec{q}, \omega), \quad (2)$$

where φ_{total} is the total potential and

$$\epsilon^{-1}(\vec{q}, \omega) = \left(1 - \frac{4\pi e^2}{(\vec{k}+\vec{G})^2}\, \alpha(\vec{k}+\vec{G}, \vec{k}+\vec{G}', \omega)\right)^{-1}_{\vec{G}_s, \vec{G}_s'}. \quad (3)$$

The momentum transfer $\vec{q}$ is unrestricted, while the vector $\vec{k}$ is confined to the first Brillouin zone and the reciprocal-lattice vector $\vec{G}_s$ is defined by $\vec{q} = \vec{k} + \vec{G}_s$.

The tensor α in Eq. (3) is the so-called polarizability tensor of the system. It is directly proportional to the response of the system to the *total* potential and is a tensor in the reciprocal-lattice vectors $\vec{G}$ and $\vec{G}'$. The tensor character of this response function simply reflects the fact that the charge induced in the system by a perturbation at wave vector $\vec{k}$ will have Fourier components at all wave vectors $\vec{k}+\vec{G}$. The tensor α must be *inverted* to obtain the inverse dielectric function and thus the scattering cross section.

In the conventional random-phase approximation (RPAB) one sets α equal to its free-electron value α^0, i.e.,[5,6]

$$\alpha^0(\vec{k}+\vec{G}, \vec{k}+\vec{G}', \omega) = \sum_{\vec{p}, l, l'} \frac{[n(l, \vec{p}) - n(l', \vec{p}+\vec{k})]\langle l, \vec{p}|e^{-i(\vec{k}+\vec{G})\cdot\vec{r}}|l', \vec{p}+\vec{k}\rangle\langle l', \vec{p}+\vec{k}|e^{i(\vec{k}+\vec{G}')\cdot\vec{r}}|l, \vec{p}\rangle}{\omega + E(l, \vec{p}) - E(l', \vec{p}+\vec{k}) + i\delta}, \quad (4)$$

where indices l and $\vec{p}$ label the energy band and crystal momentum, and $E(l, \vec{p})$ and $n(l, \vec{p})$ are the energy and occupation number, respectively, of these states. The use of Eq. (4) assumes that the

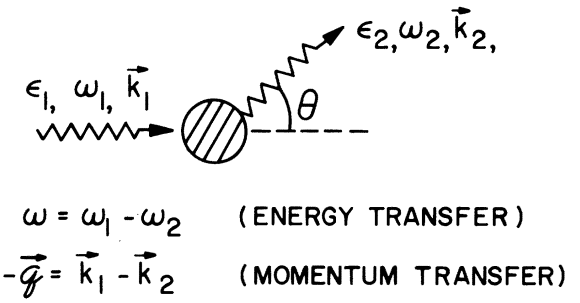

FIG. 1. Schematic diagram of a typical scattering experiment.

system responds to the total field as if it were a free inhomogeneous electron gas.

Equation (3) with the associated definition [Eq. (4)] of α^0 is quite complicated owing to the details of the band structure. However, several qualitative properties are readily apparent. (i) If the $\mathrm{Im}(\epsilon(\vec{q}, \omega))$ is small, the zeros of $\mathrm{Re}(\epsilon(\vec{q}, \omega))$ will show up as peaks in the scattering cross section. (ii) The $\mathrm{Im}(\epsilon(\vec{q}, \omega))$ arises from the vanishing of the energy denominators in Eq. (4), i.e., when

$$\omega = E(l', \vec{p}+\vec{k}) - E(l, \vec{p}). \tag{5}$$

In this case $|\vec{p}| < k_F$ and $|\vec{k}+\vec{p}| > k_F$ in the extended zone scheme. The continuum of energies defined by Eq. (5) encompasses the usual zero-momentum-transfer interband optical transitions generalized to finite $\vec{k}$.

In order to get a physical feel for the behavior of the scattering cross section we first consider the well-known homogeneous-gas RPA results. Equation (5) defines two parabolas (shown in Fig. 2),

$$\omega^{\pm} = k^2/2m \pm k v_F. \tag{6}$$

In the shaded region lying between the two parabolas, $\epsilon(\vec{k}, \omega)$ has a large imaginary part. The solution of $\epsilon(\vec{k}, \omega) = 0$, the plasmon, is shown as a dotted line. Its dispersion at long wavelengths is given by

$$\omega \approx \omega_p \left(1 + \frac{3}{10} \frac{k^2 v_F^2}{\omega_p^2}\right), \tag{7}$$

where ω_p is the free-electron plasmon frequency. The dotted curve enters the continuum at a value of momentum transfer (cutoff momentum)

$$k_c \cong \omega_p / v_F.$$

Band-structure effects modify the above picture. Qualitatively such modifications are shown in Fig. 3. In a free-electron model of the band structure, the additional parabolas reflect the presence of umklapp or equivalently interband transitions. In this simple picture, conceptually

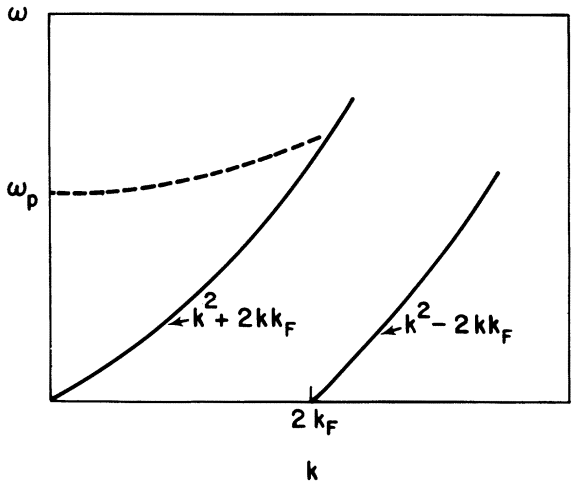

FIG. 2. Free-electron RPA excitation spectrum.

two cases are worth considering; they are labeled by (a) and (b) in Fig. 3. The first situation obtains, if the plasmon frequency is higher than the typical interband energies and if the critical momentum transfer k_c is less than $\frac{1}{2}G$, the Brillouin-zone boundary. In this case the effect of the interband transitions is to push up the plasma frequency (compared to free-electron value). The coupling to the higher plasmon branch[7] pushes the plasma frequency down. The coupling between the two branches at the zone boundary results in bending and splitting of the plasmon mode.

When the plasmon is at lower frequencies, situation (b) obtains and the plasmon is damped near $\vec{k} = 0$ and pushed down by the bulk of the interband

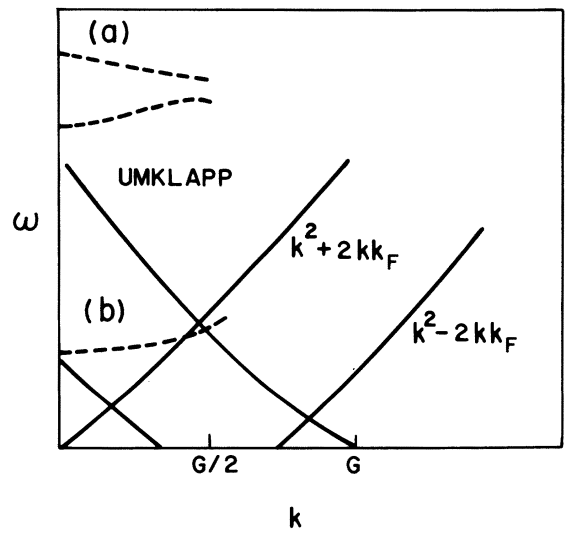

FIG. 3. Band-structure modifications of RPA excitation spectrum.

transitions above it. The bending effect will not be as well defined, since the plasmon near the zone boundary will be rather severely damped by direct, processes, as contrasted with umklapp, processes.

III. HIGH-FREQUENCY LIMIT

In many materials (for example Be with $\omega_p \approx 15$ eV) the plasma frequency is high relative to the typical interband energies, ω_B^T, so that the energy denominators in Eq. (4) may be expanded in powers of $(\omega_B^T/\omega)^2$. Each term in the power series may be evaluated by replacing the various powers of $[E(l,\vec{p}) - E(l',\vec{p}+\vec{k})]$ which appear in the expansion by commutators of the Hamiltonian H with $e^{i\vec{k}\cdot\vec{r}}$.[4] To illustrate this procedure, we look at the real part of Eq. (4) which can alternatively be written as

$$\alpha^0(\vec{k}+\vec{G},\vec{k}+\vec{G}',\omega) = -2\sum_{\vec{p}ll'} \frac{n(l,\vec{p})[E(l,\vec{p})-E(l',\vec{p}+\vec{k})]}{\omega^2-[E(l,\vec{p})-E(l',\vec{p}+\vec{k})]^2}\langle l;\vec{p}|e^{-i(\vec{k}+\vec{G})\cdot\vec{r}}|l',\vec{p}+\vec{k}\rangle\langle l',\vec{p}+\vec{k}|e^{i(\vec{k}+\vec{G}')\cdot\vec{r}}|l,\vec{p}\rangle . \tag{8}$$

Expansion in $1/\omega^2$ gives

$$\alpha^0(\vec{k}+\vec{G},\vec{k}+\vec{G}',\omega) = -2\sum_{\vec{p}ll'} \frac{n(l,\vec{p})}{\omega^2}[E(l,\vec{p})-E(l',\vec{p}+\vec{k})]\langle l,\vec{p}|e^{-i(\vec{k}+\vec{G})\cdot\vec{r}}|l',\vec{p}+\vec{k}\rangle\langle l',\vec{p}+\vec{k}|e^{i(\vec{k}+\vec{G}')\cdot\vec{r}}|l,\vec{p}\rangle$$

$$-\frac{2}{\omega^4}\sum_{\vec{p},l,l'} n(l,\vec{p})[E(l,\vec{p})-E(l',\vec{p}+\vec{k})]^3$$

$$\times\langle l,\vec{p}|e^{-i(\vec{k}+\vec{G})\cdot\vec{r}}|l',\vec{p}+\vec{k}\rangle\langle l',\vec{p}+\vec{k}|e^{i(\vec{k}+\vec{G}')\cdot\vec{r}}|l,\vec{p}\rangle + O(1/\omega^6) . \tag{9}$$

The diagonal term in Eq. (9) to order ω^{-4} can be written as

$$\alpha^0(\vec{k}+\vec{G},\vec{k}+\vec{G},\omega) = -\frac{2}{\omega^2}\sum_{\vec{p},l} n(l,\vec{p})\langle l,\vec{p}|[H,e^{-i\vec{q}\cdot\vec{r}}]e^{i\vec{q}\cdot\vec{r}}|l,\vec{p}\rangle$$

$$-\frac{2}{\omega^4}\sum_{\vec{p},l} n(l,\vec{p})\langle l,\vec{p}|[H,[H,[H,e^{-i\vec{q}\cdot\vec{r}}]]]e^{i\vec{q}\cdot\vec{r}}|l,\vec{p}\rangle , \tag{10}$$

where

$$\vec{q} = \vec{k}+\vec{G} \tag{11}$$

and H is the one-electron Hamiltonian of the system (atomic units $\hbar = e = m = 1$ will be used throughout)

$$H = \tfrac{1}{2}p^2 + V(\vec{r}). \tag{12}$$

Using the identities

$$[H,e^{-i\vec{q}\cdot\vec{r}}]e^{i\vec{q}\cdot\vec{r}} = H - H' , \tag{13}$$

and

$$[H,[H,[H,e^{-i\vec{q}\cdot\vec{r}}]]]e^{i\vec{q}\cdot\vec{r}} = H^3 - 3H^2H' + 3HH'^2 - H'^3 , \tag{14}$$

where

$$H' = \tfrac{1}{2}(\vec{p}+\vec{q})^2 + V(\vec{r}) \tag{15}$$

$$= H + \tfrac{1}{2}(q^2 - 2i\vec{q}\cdot\vec{\nabla}), \tag{16}$$

we find that Eq. (10) can be written as

$$\alpha^0(\vec{q},\vec{q},\omega) = q^2N/\omega^2 + \frac{1}{\omega^4}\sum_{l,\vec{p}} n(l,\vec{p})\langle l,\vec{p}|[(\vec{q}\cdot\vec{\nabla})^2 V]$$

$$-3q^2(\vec{q}\cdot\vec{\nabla})^2 + \tfrac{1}{4}q^6|l,\vec{p}\rangle , \tag{17}$$

where N is the average valence electronic density.

In a similar way, the leading off-diagonal term (to order ω^{-2}) is given by[4]

$$\alpha^0(\vec{k}+\vec{G},\vec{k}+\vec{G}',\omega) = \frac{(\vec{k}+\vec{G})\cdot(\vec{k}+\vec{G}')}{\omega^2}\sum_{\vec{p},l} n(l,\vec{p})$$

$$\times\langle l,\vec{p}|e^{i(\vec{G}'-\vec{G})\cdot\vec{r}}|l,\vec{p}\rangle . \tag{18}$$

Writing the effective valence-electron-ion potential (e.g., pseudopotential) as

$$V(\vec{r}) = \sum_{\vec{k}} e^{i\vec{k}\cdot\vec{r}} V_{\vec{k}} , \tag{19}$$

and the valence electronic density

$$\rho_{\vec{k}} = \sum_{l,\vec{p}} n(l,\vec{p})\langle l,\vec{p}|e^{-i\vec{k}\cdot\vec{r}}|l,\vec{p}\rangle , \tag{20}$$

Eqs. (17) and (18) can be written more conveniently as

$$\alpha^0(\vec{k}+\vec{G},\vec{k}+\vec{G},\omega)=\frac{q^2N}{\omega^2}-\frac{1}{\omega^4}\sum_{\vec{K}}(\vec{q}\cdot\vec{K})^2V_{\vec{K}}\rho_{\vec{K}} - 3\frac{q^2}{\omega^4}\sum_{l,\vec{p}}n(l,\vec{p}) \times\langle l,\vec{p}|(\vec{q}\cdot\vec{\nabla})^2|l,\vec{p}\rangle+q^6N/4\omega^4 \tag{21}$$

and for $\vec{G}\neq\vec{G}'$,

$$\alpha^0(\vec{k}+\vec{G},\vec{k}+\vec{G}',\omega)=\frac{(\vec{k}+\vec{G})\cdot(\vec{k}+\vec{G}')}{\omega^2}\rho_{(\vec{G}'-\vec{G})}. \tag{22}$$

The off-diagonal term has been calculated only to order ω^{-2}, since on inverting the dielectric tensor in Eq. (3), the leading contribution from it comes in squared (i.e., it is of order ω^{-4}).

Equations (21) and (22) are quite general. Apart from the use of RPAB, the only other approximation that has been made is that ω is large compared to typical interband energies.

The high-frequency limit (HFL) of the RPAB simplifies the expression for the various components of the dielectric polarizability tensor and illuminates the physics contained in them. In order to quantitatively discuss the collective modes in the system, we need an approximate procedure for inverting the matrix equation, Eq. (3). It is clear from Eq. (22) that under many circumstances the off-diagonal terms may be considered small. They are small at high frequencies and also whenever the crystal potential effects are small. We will assume this to be the case and work to the lowest order in the off-diagonal elements. In this case we may easily invert Eq. (3) using the formulas of Wiser [Ref. 6, Eq. (38)], i.e.,

$$\epsilon(\vec{k},\omega)=1+T_{00}(\vec{k},\omega)-\sum_{\vec{K}\neq0}\frac{T_{0\vec{K}}(\vec{k},\omega)T_{\vec{K}0}(\vec{k},\omega)}{1+T_{\vec{K}\vec{K}}(\vec{k},\omega)}. \tag{23}$$

In order to simplify the notation somewhat, we have assumed that $\vec{q}$ is in the first Brillouin zone; i.e., $G_s=0$ and $\vec{q}\equiv\vec{k}$. In Eq. (23)

$$T_{\vec{K}\vec{K}'}(\vec{k},\omega)=\frac{-4\pi e^2}{|\vec{k}+\vec{K}|^2}\alpha^0(\vec{k}+\vec{K},\vec{k}+\vec{K}',\omega). \tag{24}$$

Near the zone center the zeros of ϵ (Eq. 23) are roughly determined by the zeros of $1+T_{00}(\vec{k},\omega)$, since the off-diagonal $T_{0\vec{K}}(\vec{k},\omega)$ terms are small and $1+T_{\vec{K}\vec{K}}(\vec{k},\omega)$ is not equal to zero. Substituting the high-frequency form of $T_{00}(\vec{k},\omega)$ [see Eq. (21)] into Eq. (23) we see immediately that the leading term (ω^{-2}) in Eq. (21), when substituted into Eq. (23), yields the long-wavelength plasma frequency for the homogeneous electron gas. The next term in Eq. (21) describes the effect of the crystal potential on the long-wavelength plasma frequency. In the high-frequency approximation it is always of the same sign as the first term, i.e., it pushes the plasma frequency up, relative to its free-electron value. For a hexagonal crystal this term is, in general, anisotropic; for a cubic crystal it is isotropic, since the only tensor one can construct is δ_{ij}.

The next term in Eq. (21) yields the long-wavelength q^2 dispersion of the plasmon mode. In the absence of the periodic potential it is equal to $\frac{3}{5}N(q^4V_F^2/\omega^4)$, i.e., the usual RPA result. In the presence of band structure it may be anisotropic in other than cubic crystals. The last term contributes to the q^4 dispersion of the plasmon. There will be other terms coming from ω^{-6} terms in the diagonal pieces and ω^{-4} in the off diagonal, which also contribute to such terms so that Eq. (21) will be incomplete insofar as the q^4 corrections to the dispersion are concerned.

The summation in Eq. (23) leads to a small shift in the zeros of ϵ. This shift is simply the second-order perturbation correction to the energy of the lowest plasmon due to coupling to the higher plasmon bands. The sign of the term $[1+T_{\vec{K}\vec{K}}(0,\omega)>0]$ is positive, i.e. the other plasmons push down on the lowest plasmon near $k=0$. Near the zone boundary $\vec{k}=-\frac{1}{2}\vec{G}$, Eq. (23) is effectively a two-plasmon band model. The only term in the sum in Eq. (23) which is significant is the one with $\vec{K}=\vec{G}$. Equation (23) describes the coupling of the plasmon at $\vec{k}$ to one at $\vec{k}+\vec{K}$. While it is an approximate formula based on a weak coupling assumption (valid to second order in the coupling constant), it is exact within the framework of a two-band or single-reciprocal-lattice-vector model.[3]

Using Eq. (22) for $T_{0\vec{K}}$, the equation for the plasmon frequency ω (near $-\frac{1}{2}G$) can be written as

$$[1+T_{00}(-\tfrac{1}{2}\vec{G},\omega)][1+T_{\vec{G}\vec{G}}(-\tfrac{1}{2}\vec{G},\omega)]=(\omega_G^2/\omega^2), \tag{25}$$

where

$$\omega_G^2=4\pi e^2\rho_{\vec{G}}/m. \tag{26}$$

Since

$$T_{00}(-\tfrac{1}{2}\vec{G},\omega)=T_{\vec{G}\vec{G}}(-\tfrac{1}{2}\vec{G},\omega)\approx-\omega_p^2(\tfrac{1}{2}\vec{G})/\omega^2, \tag{27}$$

where $\omega_p(\frac{1}{2}\vec{G})$ is the plasmon frequency at $\vec{k}=\frac{1}{2}\vec{G}$, Eq. (25) becomes

$$[\omega^2-\omega_p^2(\tfrac{1}{2}\vec{G})]^2=\omega_G^4. \tag{28}$$

Thus the single plasmon mode is split at the zone boundary $\frac{1}{2}\vec{G}$ by the amount (see Fig. 3)

$$\delta = \frac{\omega_{\vec{G}}^2}{\omega_p(\frac{1}{2}\vec{G})}. \tag{29}$$

Our high-frequency picture of the plasmon is now rather complete. We have derived several general expressions which characterize the effects of band structure on the plasmon frequency and its dispersion near $\vec{k}=0$ [Eq. (21)] as well as the splitting of the plasmon mode near the zone boundary [Eq. (29)]. The only qualitative property missing from our treatment is the damping associated with umklapp processes. We will return to this point in Secs. V and VI.

IV. NEARLY-FREE-ELECTRON APPROXIMATION AND THE HIGH-FREQUENCY LIMIT

It is well known that in most solids the effective interaction of valence electrons and ions is small, i.e., the energy momentum relation is approximately $E_{\vec{k}}^0 \approx k^2/2m$ and the Fermi surface is roughly spherical in an extended zone scheme, characterized by the unperturbed Fermi function n^0. The pseudopotential theory[8] has been especially successful in treating such interactions. We will evaluate the various terms in Eqs. (21) and (29) within the framework of weak-pseudopotential approximation. This will lead to explicit expressions for the plasmon frequency, its dispersion near $\vec{k}=0$, and the splitting of the folded-back plasmons at the zone boundary. Since it is the general behavior and approximate size of these terms which are of interest to us, we will not attempt a precise calculation of them. Rather, our calculations will be limited to the second order in the "weak" pseudopotentials. In a wide class of materials such calculations are expected to be semiquantitatively correct and thus have wide applicability.

The evaluation of the second term in Eq. (21) is straightforward. Since (to the lowest order in $V_{\vec{K}}$)

$$\rho_{\vec{K}} = \frac{V_{\vec{K}}}{2\pi^2}\left[\left(\frac{K^2-4k_F^2}{4K}\right)\ln\left|\frac{K+2k_F}{K-2k_F}\right| - k_F\right], \tag{30}$$

we find that

$$\sum_{\vec{K}} (\vec{q}\cdot\vec{K})^2 V_{\vec{K}}\rho_{\vec{K}} = \frac{1}{2\pi^2}\sum_{\vec{K}} (\vec{q}\cdot\vec{K})^2 |V_{\vec{K}}|^2 \times\left[\left(\frac{K^2-4k_F^2}{4K}\right)\ln\left|\frac{K+2k_F}{K-2k_F}\right| - k_F\right]. \tag{31}$$

Similarly the next term in Eq. (21) can be written as

$$\sum_{l,\vec{p}} \langle l,\vec{p}|(\vec{q}\cdot\vec{\nabla})^2|l,\vec{p}\rangle n(l,\vec{p}) = -F\sum_{\vec{G}}\int d\vec{p}\,[\vec{q}\cdot(\vec{p}+\vec{G})]^2 n(l,\vec{p}) - F\sum_{\vec{K}\neq 0}(\vec{q}\cdot\vec{K})|V_{\vec{K}}|^2 \times\sum_{\vec{G}}\left\{\int \frac{d\vec{p}\,[\vec{q}\cdot(2\vec{p}+2\vec{G}+\vec{K})]\,n^0(\epsilon^0_{\vec{k}+\vec{G}})}{(\epsilon^0_{\vec{p}+\vec{K}+\vec{G}}-\epsilon^0_{\vec{p}+\vec{G}})^2}\right\}, \tag{32}$$

where

$$F = 3N/4\pi k_F^3. \tag{33}$$

In Eq. (32) we have assumed that the Bloch state $|l,\vec{p}\rangle$ arise from the plane wave $e^{i(\vec{p}+\vec{G})\cdot\vec{r}}$. The expression inside the curly brackets is easily evaluated and is equal to

$$\frac{\pi k_F^2}{2}\frac{(\vec{q}\cdot\vec{G})}{G^3}\left[\frac{G}{k_F}+1-\left(\frac{G^2}{4k_F^2}\right)\ln\left|\frac{G+2k_F}{G-2k_F}\right|\right]. \tag{34}$$

In the first term in Eq. (32) we cannot replace n by n^0. The change from a spherical Fermi surface will give rise to corrections of the order of $|V_{\vec{G}}|^2$ and hence must be evaluated.

In order to calculate the changes in n due to the presence of a weak pseudopotential we write

$$n = n^0 + \left(\frac{\partial n^0}{\partial\epsilon}\right)(\delta\epsilon - \delta\mu), \tag{35}$$

where

$$\frac{\partial n^0}{\partial\epsilon} = -\delta(\epsilon-\epsilon_F) \tag{36}$$

and μ is the chemical potential. Using the condition that the total number of particles is conserved, we find, to lowest order in V,

$$\delta\mu = -\frac{1}{2k_F}\sum_{\vec{G}\neq 0}\frac{|V_{\vec{G}}|^2}{|\vec{G}|}\ln\left|\frac{G+2k_F}{G-2k_F}\right|. \tag{37}$$

Working in the extended-zone scheme, the first term in Eq. (32) can be written as

$$-F\sum_{\vec{G}}\int d\vec{p}\,[\vec{q}\cdot(\vec{p}+\vec{G})]^2 n(l,\vec{p}) = D_F + D_\mu + D_\epsilon, \tag{38}$$

where

$$D_F = -F\int d\vec{k}\,(\vec{q}\cdot\vec{k})^2 n^0(\epsilon^0_{\vec{k}}), \tag{39}$$

$$D_\mu = F\int\left(\frac{\partial n^0}{\partial\epsilon}\right)(\delta\mu)[\vec{q}\cdot\vec{k}]^2\,d\vec{k}, \tag{40}$$

$$D_\epsilon = -F\int\left(\frac{\partial n^0}{\partial \epsilon}\right)(\delta\epsilon)[\vec{q}\cdot\vec{k}]^2\,d\vec{k}\,. \tag{41}$$

The first term in Eq. (32), when substituted into Eqs. (21) and (23), gives the usual q^2 plasmon dispersion for a homogeneous electron gas in the RPA. The second term arising from the change in the chemical potential is easily evaluated, the result being

$$D_\mu = (\tfrac{2}{3}\pi)\,q^2k_F^2\sum_{\vec{G}\neq 0}\frac{|V_{\vec{G}}|^2}{G}A_G, \tag{42}$$

where

$$A_G = \ln\left|\frac{G+2k_F}{G-2k_F}\right|\,. \tag{43}$$

The above correction to the q^2 dispersion is isotropic and is of such a sign as to decrease the dispersion from the free-electron RPA result. Calculation of D_ϵ is much more involved but straightforward. The result is

$$D_\epsilon = -\pi q^2k_F^2\sum_{\vec{G}\neq 0}\frac{|V_{\vec{G}}|^2}{G} \times\left\{\left[\frac{G}{k_F}+\left(1-\frac{G^2}{4k_F^2}\right)A_G\right] -\cos^2\theta\left[\frac{3G}{k_F}+\left(1-\frac{3G^2}{4k_F^2}\right)A_G\right]\right\}, \tag{44}$$

where θ is the angle between $\vec{q}$ and $\vec{G}$. The first term is isotropic while the second is not.

Equations (31)–(34) and (38)–(44) may now be substituted directly in Eqs. (21) and (22) and the dispersion relation Eq. (23) evaluated. In Table I we show a representative set of results for the pseudopotential parameters characteristic of the hexagonal metals Be and Mg. On the one hand, the plasma frequency for Be (about 20 eV) is relatively high compared to the typical interband frequencies, so that we might expect our high-frequency formulas to be accurate. On the other hand, it is known that a pseudopotential parametrization of the band structure of Be is quantitatively inadequate and that the potential is not weak. Because of this we may think of the results given in Table I as a qualitative guide (rather than a set of quantitative numbers) to the size of the correction involved. For Mg the situation is reversed. Since the pseudopotentials properly describe the energy bands[10] and are weak, we expect that our calculation of the various terms in Eq. (21) is accurate. However, the plasmon frequency (about 10 eV) is not very high relative to typical interband energies, so that we cannot expect our high-frequency formulas to be accurate.

TABLE I. Physical parameters for Be and Mg and the results for plasmon frequency in HFL.

	Be	Mg
a (Å)	2.287 [a]	3.21 [a]
c (Å)	3.583 [a]	5.21 [a]
$V_{10\bar{1}0}$ (Ry)	0.068 [b]	0.014 [c]
V_{0002} (Ry)	0.094 [b]	0.026 [c]
V_{1011} (Ry)	0.096 [b]	0.036 [c]
V_{1012} (Ry)	0.064 [b]	0.058 [c]
ω_p^F (eV)	18.44	10.89
$\omega_{pa}^{\mathrm{HFL}}$ (eV)	18.76	10.96
$\omega_{pc}^{\mathrm{HFL}}$ (eV)	18.77	10.92

[a] Reference 9.
[b] Reference 10.
[c] Reference 11.

The first two entries in the table are lattice constants along the a and c axes. The next four are the pseudopotential form factors corresponding to the smallest reciprocal-lattice vectors that give nonvanishing contributions. The lowest Fourier component (0001) does not contribute because of a vanishing structure factor. As there are no satisfactory empirical results for the pseudopotential of Be (e.g., obtained by fitting the Fermi surface), the model pseudopotential[11] of Animalu and Heine was used. For Mg, several authors have obtained pseudopotential parameters by fitting to the Fermi surface. The parameters used here are taken from the fitting by Kimball *et al.*[10] The next three entries are for the long-wavelength plasmon frequency. ω_p is the plasmon frequency for the free-electron gas of appropriate density and $\omega_{pa}^{\mathrm{HFL}}$ and $\omega_{pc}^{\mathrm{HFL}}$ are the plasmon frequency obtained in the HFL [Eqs. (21) and (23)] for momentum transfer along the a and c directions, respectively. As is clear from Eqs. (21)–(23), both the plasmon frequency and its dispersion will, in general, be anisotropic in a hexagonal crystal. Because of the many pseudopotential form factors of comparable magnitude, in this case the anisotropy tends to average out. However, in a crystal where only one of the form factors is large we may expect a significant anisotropy.

The off-diagonal terms in the dielectric constant matrix are small, justifying the use of Eq. (23). The diagonal term in Eq. (21) pushes the plasmon mode higher in energy while the off-diagonal contribution in Eq. (21) pushes it down, the former being about 10 times larger than the latter in magnitude. The correction to the q^2 dispersion coefficient for the plasmon from the free-electron value calculated in the HFL for the plasmon in the a and c direction are, respectively, $\sim+10^{-3}$ and -10^{-3} (a. u.) for both Be and Mg. This is quite sensitive to the relative strengths of the various pseudopotential coefficients. Again the small anisotropy in dispersion is due to the fact that many pseudopotential coefficients give sig-

nificant contributions that tend to cancel. It should be remarked that in order to compare our results with the recent experiment[1] on Be, we must make the correction to the plasmon frequency arising from core polarization. The correction is -0.22 and -0.51 eV to the plasmon frequency for Be and Mg, respectively. With the above correction, the results compare favorably with experiment.[1] The anisotropy in the dispersion has the correct sign; however, it is much too small compared to the experimental values.

V. GENERAL WEAK PSEUDOPOTENTIAL APPROXIMATION

To the lowest order in the crystal potential, Eq. (23) is a valid representation of the dielectric constant, independent of the use of the high-frequency approximations. The advantages of the HFL is its intrinsic simplicity. However, the use of a more general expression like Eq. (23) enables us to extend our calculations to materials where the plasma frequency is comparable to typical interband energies, i.e., there is appreciable oscillator strength left at these energies. In addition, we can begin to include effects such as damping and dispersion away from the zone center.

The expression for the real part of $\epsilon(0,\omega)$ in this weak pseudopotential approximation has been given by Wiser [Ref. 6., Eq. (39)]. This equation can be written in a more convenient form as

$$\epsilon(0,\omega)=1-\left(\frac{\omega_p^f}{\omega}\right)^2+\frac{2}{\pi^2\omega^2}\sum_{\vec{G}}{}'\,|V_{\vec{G}}|^2|G^\mu|^2 I_1^G - \left(\frac{2}{\pi^2}\right)^2\sum_{\vec{G}}{}'\,\frac{|V_{\vec{G}}|^2|G^\mu|^2(I_1^G)^2}{G^2+(2/\pi^2)(I_{-1}^G)}, \tag{45}$$

where G^μ is the component of $\vec{G}$ in the direction of the momentum transfer and

$$I_n^G=\sum_{\vec{G}'}\int d\vec{k}\,\frac{n(E_{\vec{k}+\vec{G}'})}{(\Delta\epsilon_{\vec{G}}^{\vec{}})^n[(\Delta\epsilon_{\vec{G}}^{\vec{}})^2-\omega^2]} \tag{46}$$

and

$$\Delta\epsilon_{\vec{G}}^{\vec{}}=(E_{\vec{k}+\vec{G}+\vec{G}'}-E_{\vec{k}+\vec{G}'})\,. \tag{47}$$

$E_{\vec{k}+\vec{K}}$ is the band energy corresponding to the wave vector $\vec{k}$ inside the Brillouin zone and the band labeled by the reciprocal-lattice vector $\vec{K}$; $n(E_{\vec{k}})$ is the Fermi distribution function. To the lowest order in the pseudopotential we get

$$I_1^G=(\pi/2G\omega^2)[F(\tfrac{1}{2}G^2+k_FG)-F(\tfrac{1}{2}G^2-k_FG)], \tag{48}$$

where

$$F(X)=2X(1-X/G^2)\ln|X| + \frac{X^2-\omega^2-XG^2}{G^2}\ln|X^2-\omega^2| - \omega\ln\left|\frac{X+\omega}{X-\omega}\right| \tag{49}$$

and

$$I_{-1}^G=(\pi/2G)[P(\tfrac{1}{2}G^2+k_FG)-P(\tfrac{1}{2}G^2-k_FG)], \tag{50}$$

where

$$P(X)=\frac{(X^2-\omega^2-XG^2)}{G^2}\ln|X^2-\omega^2| + (2X-X^2/G^2)-\omega\ln\left|\frac{X+\omega}{X-\omega}\right|\,. \tag{51}$$

The damping of the long-wavelength plasmon, given by $\mathrm{Im}\epsilon(\vec{k},\omega)=\epsilon_2(\vec{k},\omega)$, is governed mainly by the second term in Eq. (23). We will show that in the weak pseudopotential approximation its contribution to $\epsilon_2(0,\omega)$ is of the order of V_G^2; that of the last term, or the local-field term, is of the order of V_G^4 and hence can be ignored. Using the small-q expansion for the matrix element in Eq. (4)

$$|\langle l,\vec{k}|e^{-i\vec{q}\cdot\vec{r}}|l',\vec{k}+\vec{q}\rangle|^2=\delta_{ll'}+(1-\delta_{ll'})|P_{ll'}|^2, \tag{52}$$

where

$$|P_{ll'}|^2=\frac{|\langle l,\vec{k}|\vec{q}\cdot\vec{p}|l',\vec{k}\rangle|^2}{[E(l,\vec{k})-E(l',\vec{k})]^2} \cong q^2\frac{[(\vec{G}'-\vec{G})^\mu]^2|V_{(\vec{G}'-\vec{G})}|^2}{(E^0_{\vec{k}+\vec{G}'}-E^0_{\vec{k}+\vec{G}})^4}\,. \tag{53}$$

The contribution to $\epsilon_2(\vec{q},\omega)$ from the second term in Eq. (23) can be written as

$$\epsilon_2(\vec{q},\omega)\cong\left(\frac{e^2}{q^2\pi}\right)\sum_l\int d\vec{k}\,n(l,\vec{k})[\delta(E(l,\vec{k}+\vec{q})-E(l,\vec{k})-\omega)-\delta(E(l,\vec{k}-\vec{q})-E(l,\vec{k})+\omega)] + \left(\frac{e^2}{\pi q^2}\right)\sum_{ll'}{}'\int d\vec{k}[n(l,\vec{k})-n(l',\vec{k})]\,\delta(E(l',\vec{k})-E(l,\vec{k})-\omega)\,|P_{ll'}|^2\,. \tag{54}$$

It is clear from Eq. (54) that when ω is higher than the conduction bandwidth, the first term, corresponding to the one-electron intraband transitions, cannot contribute to the plasmon damping. However, in a metal it will give the main contribution when ω is smaller than the interband

TABLE II. Band-structure effect on the plasmon frequency in Li and Na.

	Li	Na
a (Å)	3.49	4.23
V_{110} (Ry)	0.11 [a]	0.02 [b]
ω_p^f (eV)	8.05	5.95
ω_p^{BS} (eV)	7.49	5.90

[a] Reference 12.
[b] Reference 13.

energy. This term will be identically zero for an insulator.

Using Eq. (53) and taking ω large, Eq. (54) can, after some manipulation, be written as

$$\epsilon_2(0,\omega)=\frac{e^2}{\omega^4}\sum_{\vec{G}}|V_{\vec{G}}|^2\frac{|G^\mu|^2}{G^3}\times[k_F^2G^2-(\omega-\tfrac{1}{2}G^2)^2] \quad (55)$$

Here $\vec{G}$ is restricted, so that $k_F^2>(1/G^2)(\omega-\frac{1}{2}G^2)^2$.

Equations (45)–(47) can be used to calculate the plasmon frequency, while Eq. (55) can be used to calculate its damping. These equations have been applied to the case of Li and Na. The results (along with the parameters used) are shown in Table II.

The first entry in the table gives the lattice constant, and the second the pseudopotential parameter used. Only one coefficient, namely (110), is used, since we are interested in a typical band-structure effect and not a detailed calculation. The pseudopotential parameter was obtained by fitting the Fermi surface.[12,13] The next two entries ω_p^f and ω_p^{BS} are the plasmon frequency in the free-electron approximation and the one including the band-structure effect using Eqs. (45)–(51). While the shift of the plasmon frequency in Li is appreciable, it is negligible in Na. This is not surprising in view of the very weak pseudopotential for Na. Before comparing to the experimental result, one must correct for core polarization. The effect of core polarization on the plasmon frequency are -0.37 eV and -0.06 eV for Na and Li, respectively. The results for the damping are not tabulated. It is clear from Eq. (55) that $\epsilon_2 \sim V_G^2/\omega_p^2$ and in Li this ratio is ~0.01. Thus this simple treatment of band-structure effects on plasmons gives a shift, in rough agreement with experiment and gives a free-damping coefficient, at $q=0$ which is much too small relative to the experimental numbers.

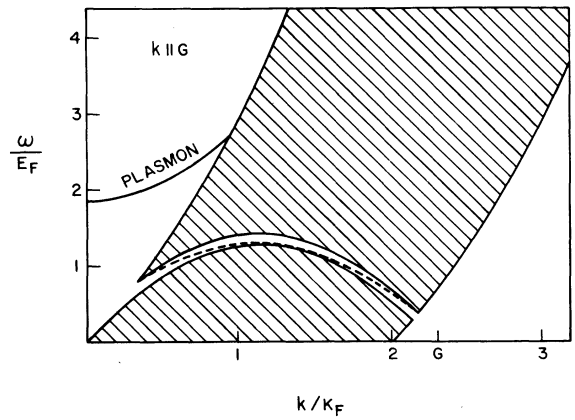

FIG. 4. Energy of excitations shown as a function of momentum. Shaded area shows the single-particle excitation continuum. The dashed line located in the gap of the continuum represents the zone boundary collective state.

VI. TWO-BAND MODEL

In 1968 Foo and Hopfield[3] presented a simplified one-reciprocal-lattice-vector model of the response function of Bloch electrons in the solid. The calculation was done in RPA and they arrived at an expression for the dielectric function identical to Eq. (23) with only a single term in the sum. The electronic energy denominators in the expressions for T_{00} and $T_{0\vec{G}}$, because of the single-reciprocal-lattice vector assumption, had a particularly simple analytical form characteristic of a two-band model. Besides the simplifications introduced by such a model, several unusual and unrealistic features were also present. In particular, the pair-excitation spectrum (see Fig. 4), because of the one-dimensional nature of the model, developed a gap in it. This gap led, in a natural way, to an additional undamped plasmon-like mode. This low-lying longitudinal mode will surely be strongly damped in any real crystal where by virtue of the crystal symmetry such a two-band model is inadequate. For example, in Li there are twelve equivalent $\langle 110\rangle$ reciprocal-lattice vectors and they will enter into the bands in certain symmetrized combinations. However, the simplicity of this model permits a complete calculation of the effect of the periodic potential on the loss spectrum, including damping and dispersion.

In Figs. 5 and 6 we present some numerical results for this model. Figure 5 shows the real plasmon dispersion for an unrealistic set of parameters, i.e., $\omega_p/E_F=11.0$ and $G/k_F=2.0$. We choose these parameters to force the plasmon out of the umklapp continuum and to position the zone boundary, at $\frac{1}{2}G$, considerably below the critical momentum k_c [Eq. (6)]. In this case the plasmon is always undamped and the spectrum is

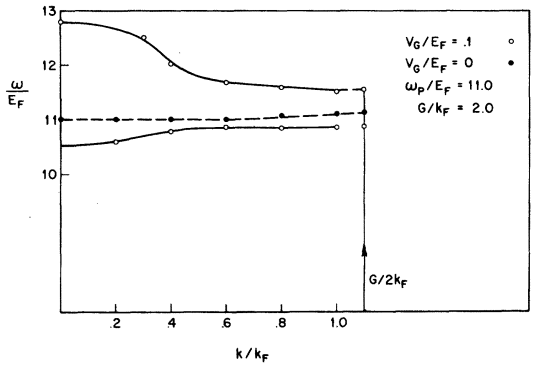

FIG. 5. Plasmon dispersion in the one-dimensional model of Ref. 6, with $\omega_p/E_F = 11.0$, $G/k_F = 2.2$, $V_G/E_F = 0.1$, and $V_G/E_F = 0$.

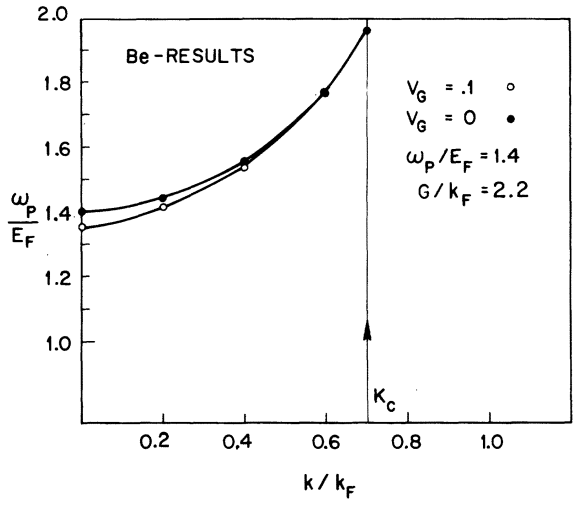

FIG. 6. Plasmon dispersion in the one-dimensional model of Ref. 6; with $\omega_p/E_F = 1.4$, $G/k_F = 2.0$, $V_G/E_F = 0.1$, and $V_G/E_F = 0$.

quite similar to that sketched in Fig. 3(a). The RPA plasmon position is shown by the dotted curve. The zone-boundary splitting of $0.7E_F$ is consistent with Eq. (29).

In Fig. 6 we have plotted the plasmon dispersion and damping for a set of parameters characteristic of Be. The situation here is quite different. The plasmon is damped near $k = 0$ and in the neighborhood of the zone boundary the plasmon has already entered into the continuum, i.e., $k_c < \frac{1}{2}G$, so that the spectrum has lost much of its sharply peaked character. If we persist in plotting the peak position, we see that [contrary to the prediction of Eq. (29)] the location at this peak is in good agreement with the simple RPA prediction. Equation (29) would predict a depression of approximately $0.2E_F$. The reason for this apparent contradiction is that damping effects change the nature of plasmons near the zone boundary. This is the reason that Eq. (29) gives good results in the first case, where damping effects are negligible.

VII. CONCLUSIONS

The effects of band structure on the behavior of collective modes in metals and thus on the dynamic structure factor are rather detailed and quite complicated. It would be important and extremely useful to have a detailed RPA calculation of the dynamic structure factor which includes, in detail, band-structure effects. However, in the absence of such a calculation, our study, based on rather general consideration, has revealed a number of qualitative features. In general, these effects are quite small, even in materials where the one-electron spectrum is not very free-electron-like. The numerical reason for this is simply that band-structure effects come in as the square of some pseudopotential divided by an energy which is characteristically of the order of the full bandwidth. Thus, even in the most favorable cases, band-structure effects will typically modify the free-electron spectrum of most simple metals by a few percent.

Experimentally[1] the spectrum seems to deviate from simple (no band structure) RPA-type calculations by much larger amounts. In fact, in many cases, the spectrum is qualitatively different from what we expect. These differences probably arise from a combination of lattice periodicity and strong spatial correlations of electrons in the fluid due to their Coulomb interactions. Such effects have been completely neglected in our present treatment and await inclusion into a more complete formulation of the problem.

---

*Resident visitor from the Dept. of Physics, Columbia University, New York, N. Y. 10027.

[1]P. Eisenberger, P. M. Platzman, and K. C. Pandey, Phys. Rev. Lett. 31, 311 (1973).
[2]M. S. Haque and K. L. Kliewer, Phys. Rev. B 7, 2416 (1973); J. P. Walter and M. L. Cohen, Phys. Rev. B 5, 3101 (1972).
[3]E-Ni Foo and J. J. Hopfield, Phys. Rev. 173, 635 (1968).
[4]P. M. Platzman and P. A. Wolff, *Waves and Interactions in Solid State Plasmas* (Academic, New York, 1973).
[5]S. L. Adler, Phys. Rev. 126, 413 (1962).
[6]N. Wiser, Phys. Rev. 129, 62 (1963).
[7]W. M. Saslow and G. F. Reiter, Phys. Rev. B 7, 2995 (1973).

[8]M. L. Cohen and V. Heine, Solid State Phys. 24, 37 (1970).
[9]R. W. G. Wyckoff, *Crystal Structures* (Interscience, New York, 1951), Vol. I.
[10]J. C. Kimball, R. W. Stark, and F. M. Mueller, Phys. Rev. 162, 600 (1967).
[11]A. O. E. Animalu and V. Heine, Philos. Mag. 12, 1249 (1965).
[12]J. J. Donaghy and A. T. Stewart, Phys. Rev. 164, 391 (1967).
[13]M. J. G. Lee, Proc. R. Soc. A 295, 440 (1966).